Predicting excitonic gaps of semiconducting single-walled carbon nanotubes from a field theoretic analysis

Robert M. Konik,[1] Matthew Y. Sfeir,[2] and James A. Misewich[1]

[1]*Condensed Matter Physics and Material Science Department, Brookhaven National Laboratory, Upton, New York 11973, USA*

[2]*Center for Functional Nanomaterials, Brookhaven National Laboratory, Upton, New York 11973, USA*

(Received 9 March 2014; revised manuscript received 16 December 2014; published 17 February 2015)

We demonstrate that a nonperturbative framework for the treatment of the excitations of single-walled carbon nanotubes based upon a field theoretic reduction is able to accurately describe experiment observations of the absolute values of excitonic energies. This theoretical framework yields a simple scaling function from which the excitonic energies can be read off. This scaling function is primarily determined by a single parameter, the charge Luttinger parameter of the tube, which is in turn a function of the tube chirality, dielectric environment, and the tube's dimensions, thus expressing disparate influences on the excitonic energies in a unified fashion. We test this theory explicitly on the data reported by Dukovic *et al.* [Nano Lett. **5**, 2314 (2005)] and Sfeir *et al.* [Phys. Rev. B **82**, 195424 (2010)] and so demonstrate the method works over a wide range of reported excitonic spectra.

DOI: 10.1103/PhysRevB.91.075417 PACS number(s): 73.63.Fg, 02.70.−c, 11.10.Kk, 78.67.Ch

I. INTRODUCTION

One of the most challenging problems in studying low dimensional strongly correlated systems is the quantitative prediction of the absolute values of the energies of its fundamental excitations. These energies are typically nonperturbative in nature and so lie out of the reach of approximations that treat interactions as weak. One nonperturbative theoretical tool that is not so limited is quantum field theory. Quantum field theories arise as descriptions of condensed matter systems by focusing on their low energy properties. They have had considerable success in studying a number of problems in quantum magnetism [1–7], in particular the remarkable prediction of an E_8 symmetry in a critical quantum Ising model in a longitudinal field [8] that has been recently observed [9], one dimensional Mott insulator physics [10–13], and Luttinger liquids in all of their various forms [14–20]. However, quantum field theories are best at predicting universal properties of materials. Typically they do not attempt to understand absolute values of gap energies, but instead are satisfied with (the still very nontrivial task of) computing ratios of excitation energies.

In this paper we show that this restriction need not always hold. We demonstrate that the data that can be extracted from a field theoretic analysis can in fact be used to predict the absolute magnitude of excitation gaps. To this end we analyze a field theoretic treatment of the excitonic spectrum of semiconducting carbon nanotubes [21]. This spectrum determines the optical properties of carbon nanotubes and so determines their use in various optical-electronic devices such as solar cells [22]. The excitonic gaps of semiconducting carbon nanotubes are known to be variegated, depending on tube diameter, chirality, subband, and dielectric environment [23–29]. They are also known to be strongly renormalized by Coulomb interactions from their bare, noninteracting values [25,30–33]. Both of these features make them an ideal testing ground for the analysis presented herein. While we apply this analysis to carbon nanotubes, the ideas behind it apply equally well to other one dimensional (1D) strongly correlated nanomaterials such as carbon nanoribbons [34], boron nitride nanotubes [35], and excitons in semiconducting quantum wires [36].

Typically, excitonic spectra of carbon nanotubes have been determined using a Bethe-Salpeter equation combined with first principle input [31,32,37–39]. While this methodology results in an estimate for the absolute magnitude of an excitonic gap, it does so by focusing upon a particular subband of a tube of a particular chirality and in a particular dielectric environment. In our field theoretic treatment of excitonic spectra, even though we are interested in the absolute values of gaps, we are still able to derive a universal scaling function from which the values of the excitonic gaps can be read off. The key parameter of this scaling function will be the total charge Luttinger parameter, K_{c+}, a measure of the effective strength of Coulomb interactions in the tube [19,33].

This paper is organized as follows. In Sec. II we both review and extend the field theoretic treatment of excitons in carbon nanotubes presented in Ref. [21]. In particular the new theoretical ingredients found in this paper are an identification of how the effective bandwidth (or cutoff) in the field theory depends on the physical parameters of the nanotubes as well as a full derivation of the corrections due to this finite bandwidth to the excitonic gaps. It is here then that we derive a universal scaling function for the excitonic gaps. In Sec. III we compare the results coming from this theoretical treatment to actual excitonic data coming from a wide range of tubes. We demonstrate a good match between theory and experiment. Finally in Sec. IV we draw conclusions and discuss future directions.

II. FIELD THEORETIC APPROACH

We begin by reviewing our field theoretical treatment presented in Ref. [21]. In this treatment we focus on a single subband of a carbon nanotube. In Appendix C we argue that intersubband interactions lead only to very weak perturbations on the spectra of a single subband. This subband at low energies is described by four sets of right ($r = +$) and left ($r = -$) moving fermions, $\psi_{r\alpha\sigma}$ (two for the spin, σ, degeneracy and

 ©2015 American Physical Society

two for the valley, $\alpha = K, K'$, degeneracy). These fermions have a Hamiltonian given by

$$H = \int dx(\mathcal{H}_{\rm kin} + \mathcal{H}_{\rm gap}) + H_{\rm Coulomb}. \quad (1)$$

The first part of this Hamiltonian, $\mathcal{H}_{\rm kin} + \mathcal{H}_{\rm gap}$, describes noninteracting fermions with a band dispersion of $\epsilon^2(p) = v_0^2 p^2 + \Delta_0^2$:

$$\mathcal{H}_{\rm kin} = i v_0 \sum_{r\alpha\sigma} r \psi^\dagger_{r\alpha\sigma} \partial_x \psi_{r\alpha\sigma};$$
$$\mathcal{H}_{\rm gap} = \Delta_0 \sum_{r\alpha\sigma} \psi^\dagger_{r\alpha\sigma} \psi_{-r\alpha\sigma}, \quad (2)$$

where v_0 is the bare velocity of the fermions.

$H_{\rm Coulomb}$, on the other hand, encodes the interactions in the tube. We only consider the strongest part of this interaction, a forward scattering term given by

$$H_{\rm Coulomb} = \frac{1}{2}\int dx dx' \rho(x) V_0(x - x') \rho(x'),$$

where $\rho(x) = \sum_{r\alpha\sigma} \psi^\dagger_{r\alpha\sigma}(x)\psi_{r\alpha\sigma}(x)$. A precise enumeration of the other terms arising from $H_{\rm Coulomb}$ are given in Ref. [19]. However, we have checked that these terms only affect weakly (at the 1% level) the values of the excitonic gaps.

To treat this model we regroup terms in this Hamiltonian. We, as per normal, do not treat $H_{\rm Coulomb}$ as a perturbation of the noninteracting Hamiltonian $\int dx(\mathcal{H}_{\rm kin} + \mathcal{H}_{\rm gap})$. Instead we treat $\int dx \mathcal{H}_{\rm gap}$ as a perturbing term of $\int dx \mathcal{H}_{\rm kin} + H_{\rm Coulomb}$. In this picture the "unperturbed" Hamiltonian is nothing more than the Hamiltonian of a metallic carbon nanotube while $\mathcal{H}_{\rm gap}$ is treated as a confining interaction on top of the metallic tube. We can make progress here through bosonization.

The interacting metallic tube has an extremely simple form under bosonization [19,20]. Introducing the chiral bosons $\phi_{r\alpha\sigma}$ (see Appendix A for our bosonization conventions), we can write the right and left moving fermions via

$$\psi_{r\alpha\sigma} \sim \exp(i\phi_{r\alpha\sigma}). \quad (3)$$

Once this is done, we arrive at a theory of four Luttinger liquids described by the four bosons $\theta_i, i = c_\pm, s_\pm$ (and their duals ϕ_i),

$$H_0 = \int dx \sum_i \frac{v_i}{8\pi}\left(K_i(\partial_x\phi_i)^2 + K_i^{-1}(\partial_x\theta_i)^2\right). \quad (4)$$

These four bosons $\theta_i, i = c_\pm, s_\pm$ are linear combinations of the original four bosons. These combinations separate out charge and flavor degrees of freedom in the tube. For our purposes the most significant boson is the total charge boson,

$$\theta_{c+} = \sum_{r=\pm} \frac{r}{2}(\phi_{rK\uparrow} + \phi_{rK\downarrow} + \phi_{rK'\uparrow} + \phi_{rK'\downarrow}), \quad (5)$$

as it is the only boson to see the effects of the Coulomb interaction. In particular, the charge Luttinger parameter, K_{c+}, and the charge velocity, $v_{c+} = v_0/K_{c+}$, are strongly renormalized while the remaining three Luttinger parameters are equal to 1.

For long range Coulomb interactions [19], K_{c+} has the form

$$K_{c+} = \left(1 + \frac{8e^2}{\pi\kappa\hbar v_0}[-\log(k_{\rm min}R) + c_0]\right)^{-1/2}. \quad (6)$$

This expression for K_{c+} takes into account all of the key identifiers of the tube. κ is the dielectric constant of the medium surrounding the tube and is the factor that determines most strongly the effective strength of the Coulomb interaction, i.e., how much K_{c+} deviates from 1. $k_{\rm min}$ is the minimum allowed wave vector in the tube. It necessarily has to be larger than $2\pi/L$ where L is the length of the tube, but can in principle be much larger, say on the order of the inverse mean free path in the tube. R is the tube's radius and finally c_0 is a wrapping vector [the vector (n,m) that identifies how a graphene sheet is rolled up to form a particular tube] dependent $O(1)$ constant whose derivation can be found in Refs. [18] and [19]. In typical nanotubes, K_{c+} can take on values in the range of $\sim$0.2.

Having bosonized H_0 we now turn to the bosonization of $\mathcal{H}_{\rm gap}$. Under bosonization this term takes on a sine-Gordon-like form, i.e.,

$$\mathcal{H}_{\rm gap} = \frac{4\tilde{\Delta}_0}{\pi}\left[\prod_i \cos\left(\frac{\theta_i}{2}\right) + \prod_i \sin\left(\frac{\theta_i}{2}\right)\right], \quad (7)$$

where $\tilde{\Delta}_0 = \Delta_0(\Lambda)(\Lambda/v_{c+})^{(1-K_{c+})/4}$ and Λ is the effective bandwidth of the tube [40]. As we stressed in Ref. [21], this renormalization of the gap has important consequences for the excitonic physics of the tube. In field theoretic language, the coupling Δ_0, has picked up an anomalous dimension. Rather than purely having the dimensions of energy, $\tilde{\Delta}_0$ now has the dimensions of energy$^{(5-K_{c+})/4}$ $\times$ velocity$^{(K_{c+}-1)/4}$. This means that all excitation gaps of the tube no longer linearly scale with $\tilde{\Delta}_0$ but scale rather with the nontrivial power $\tilde{\Delta}_0^{4/(5-K_{c+})}$. Coupling constants (here the bare gap) inheriting "anomalous dimensions" is a standard feature of quantum field theories. These anomalies allow one to easily access aspects of nonperturbative physics: An immediate consequence of this was argued in Ref. [21] to be that the ratio of excitons between the first and second subbands goes as $2^{4/(5-K_{c+})}$ (not 2 as predicted by noninteracting band theory), so providing a straightforward resolution of what Ref. [33] termed the exciton ratio problem.

In the above we have written the bare gap as $\Delta_0 = \Delta_0(\Lambda)$ to indicate that this bare gap has a cutoff dependence. In our calculations we will always import the value of this bare gap from a tight-binding description of the nanotube of concern. But it is important to stress (as will be apparent in the next section) that any tight-binding description has this built-in cutoff (which is related to the bandwidth of the model).

Derivation of a scaling form for excitonic gaps

In this section we go beyond this basic characterization of scaling in the theory and develop a scaling function for the gap able to predict gap magnitudes with good quantitative accuracy. An important part of this development will be to understand how corrections induced by the presence of a finite cutoff, Λ, affect the end predictions of the gap magnitude. In a treatment of the tubes as a tight-binding lattice model, this would always be implicit as the cutoff would be found in the various lattice parameters (for example, the hopping amplitudes of the model). But because we are working in a continuum reduction, we have to make the effects of the cutoff explicit. As will be seen, we will also have to worry about how

to connect the cutoff of the physical system with the cutoff present in our numerical treatment of the continuum model.

We begin the development of the scaling function by using dimensional analysis. This tells us that the gap, E_α, of any excitation α (exciton, single particle, or otherwise) takes the following universal form:

$$E_\alpha = f_\alpha^\Lambda(K_{c+})\tilde{\Delta}_0^{4/(5-K_{c+})} v_{c+}^{\mu(K_{c+})}, \tag{8}$$

with $\mu(K_{c+}) = (1-K_{c+})/(5-K_{c+})$ and where $f_\alpha^\Lambda(K_{c+})$ is some dimensionless function. We want to stress that this form is nonperturbative and does not depend on the strength of the bare gap Δ_0. This fact derives from the anomalous scaling dimension of the renormalized coupling $\tilde{\Delta}_0$ appearing in $\mathcal{H}_{\text{gap}}$, being *exactly* $3/4 + K_{c+}/4$. The anomalous dimension of this coupling arises from the normal ordering of the cosine operator. This normal ordering removes all UV divergences [40] in the model and so the anomalous dimension of the operator is the same regardless of the value of Δ_0. In general when considering a massless $1+1$D field theory (here the metallic carbon nanotube) perturbed by a relevant operator (here $\mathcal{H}_{\text{gap}}$), the anomalous dimension of the perturbing operator is unchanged (and so is a nonperturbative quantity) when this dimension is less than 1 (as is the case here) because in such cases the theory is completely UV finite (i.e., there are no UV divergences which might lead to further changes in the perturbing operator's anomalous dimension) [41].

The dimensionless scaling function has the general form

$$f_\alpha^\Lambda(K_{c+}) = f_\alpha^\infty(K_{c+})\left[1 + A(K_{c+})\left(\frac{\tilde{\Delta}_0}{v_0}\right)^2\left(\frac{v_0}{\Lambda}\right)^{(5-K_{c+})/2}\right]. \tag{9}$$

$f_\alpha^\infty(K_{c+})$ governs the gap in the large bandwidth, $\Lambda \gg \Delta_0$, limit and was already determined in Ref. [21]. However, not previously considered, the scaling function sees corrections at finite bandwidth. These corrections will be important for predicting accurately the excitonic gaps of excitons in the higher subbands. The constant $A(K_{c+})$ is a dimensionless parameter (but depends on the charge Luttinger parameter) that governs the size of these corrections. It is plotted in Fig. 2(a). The form of $A(K_{c+})$ is derived in what follows.

To begin to derive the form of the scaling function in Eq. (9), we will first consider the effects of the cutoff on the excitation spectrum in the context of a particular regulation scheme. The scheme, a numerical one, goes under the name TCSA-NRG (truncated conformal spectrum approach with a numerical renormalization group) [21]. It is an extension of the TCSA developed in Ref. [42] in that it adds a numerical renormalization group procedure modeled after the one developed by Wilson [43] to study quantum impurity problems. We will first detail how the cutoff as implemented in the numerics effects gaps and then turn to how to connect the numerical cutoff with the cutoff of the actual system, the carbon nanotube.

TCSA-NRG is able to study any Hamiltonian which can be written as a perturbed conformal field theory:

$$\mathcal{H} = \mathcal{H}_{\text{CFT}} + \lambda\Phi_{\text{perturbation}}, \tag{10}$$

where here in this case $\mathcal{H}_{\text{CFT}}$ is a theory of four bosons, θ_i, the coupling λ equals $4\tilde{\Delta}_0/\pi$, and $\Phi_{\text{perturbation}} = [\prod_{i=1}^4 \cos(\theta_i/2) + \prod_{i=1}^4 \sin(\theta_i/2)]$. The method uses the Hilbert space of $\mathcal{H}_{\text{CFT}}$ as a computational basis. (For details of the case at hand, see Refs. [21] and [44].) This computational basis is optimal because the exact computation of matrix elements of $\Phi_{\text{perturbation}}$ is readily done using the commutation relations of the governing algebra of the unperturbed conformal theory, the Virasoro algebra. Being able to compute these matrix elements means $\mathcal{H}$ can be recast as a matrix. For this matrix to be a finite matrix, we need to truncate the Hilbert space of $\mathcal{H}_{\text{CFT}}$. The unperturbed energies of the eigenstates of $\mathcal{H}_{\text{CFT}}$, $\{|\beta\rangle\}$, appearing in the excitonic sector have the form

$$E_\beta = \sum_{i=1}^4 \frac{v_0}{K_i}\left(\frac{2\pi n_i}{L_{TCSA}} - \frac{c}{12L_{TCSA}}\right), \tag{11}$$

where the n_i are integers and c is the central charge of a single boson ($c=1$). Here L_{TCSA} is the length of the system used in the numerics and is to be distinguished both from the radius, R, of the nanotube and the length, L, of the tube. We do not have to choose L_{TCSA} to be equal to L. One of the features of this numerical scheme is that finite size effects are exponentially small (provided the system has a finite gap) and so typically we work in a regime where $L_{TCSA} \ll L$ but $L_{TCSA}\Delta_0 \gg 1$.

To implement the cutoff in the numerics we insist that the integers, n_i, appearing in Eq. (11) satisfy

$$\sum_i (n_i/K_i) \leqslant N.$$

This allows us to define the cutoff of this method as

$$\Lambda_{TCSA} = v_0\frac{2\pi N}{L_{TCSA}}, \tag{12}$$

where N is some integer.

With this in hand, the next step in the derivation of the scaling form is to write down the β function of the coupling constant $\tilde{\Delta}_0$ that governs the size of the gaps. Manipulation of this β function will allow us to write down the scaling form for the gap that appears in Eq. (9). The β function has the form

$$N\frac{d\tilde{\Delta}_0}{dN} = \alpha(K_{c+})\frac{\tilde{\Delta}_0^3}{v_0^2}\left(\frac{L_{TCSA}}{2\pi N}\right)^{(5-K_{c+})/2} + O\left[\tilde{\Delta}_0^5\left(\frac{L_{TCSA}}{N}\right)^{5-K_{c+}}\right]. \tag{13}$$

Now this β function is written down to lowest order in Δ_0. However, higher order terms in the β function are suppressed by powers of $\Lambda_{TCSA}^{-(5-K_{c+})/2}$ and as we are interested in the correction that comes from having a large but finite cutoff in the theory, this order is sufficient for our purposes. In principle the numerical coefficient $\alpha(K_{c+})$ can be determined analytically. This, however, is complicated in this case because we have a theory of four bosons whose velocities are not all the same. As such we will extract it numerically from the TCSA data. This numerical determination is what is used to plot $A(K_{c+})$ in Fig. 2(a). The form this β function has can be determined following Refs. [45] and [46] by insisting that the partition function of the theory remains invariant under changes in the

cutoff Λ_{TCSA}. In the gapped phase of the theory with L_{TCSA} sufficiently large this is equivalent to insisting the gaps of the theory are invariant under the renormalization group (RG) flow.

If we integrate this β function we obtain an expression relating the coupling in the absence of a cutoff to that with a cutoff:

$$\tilde{\Delta}_0(N=\infty) = \frac{\tilde{\Delta}_0(N)}{1 - \frac{2\alpha(K_{c+})}{5-K_{c+}} \frac{\tilde{\Delta}_0^2(N)}{v_0^2} \left(\frac{L_{TCSA}}{2\pi N}\right)^{(5-K_{c+})/2}}. \quad (14)$$

This relation tells us how to obtain the same numerical values for the gaps, E_α, from two different theories: one with no cutoff and a value of $\tilde{\Delta}_0 = \tilde{\Delta}_0(N=\infty)$, and one with a finite cutoff $\Lambda_{TCSA} = 2\pi N/L_{TCSA}$ and $\tilde{\Delta}_0 = \tilde{\Delta}_0(N)$ where $\tilde{\Delta}_0(\infty)$ and $\tilde{\Delta}_0(N)$ are related by the above equation.

The gaps, E_α, in the absence of a cutoff, depend on the coupling $\tilde{\Delta}_0(\infty)$ via the relation

$$E_\alpha(N=\infty, \tilde{\Delta}_0 = \tilde{\Delta}_0(\infty)) = f_\alpha^\infty \tilde{\Delta}_0(\infty)^{4/(5-K_{c+})}, \quad (15)$$

a simple consequence of dimensional analysis (taking into account the anomalous dimensions of the coupling constant, $\tilde{\Delta}_0$). By the RG invariance just described, we have $E_\alpha(N=\infty, \tilde{\Delta}(\infty)) = E_\alpha(N, \tilde{\Delta}(N))$. So substituting this into Eq. (15) and using Eq. (14) we obtain the desired scaling form:

$$E_\alpha(N, \tilde{\Delta}_0(N)) = f_\alpha^\infty (\tilde{\Delta}_0(N))^{4/(5-K_{c+})} \left[1 + \frac{8\alpha(K_{c+})}{(5-K_{c+})^2} \times \left(\frac{\tilde{\Delta}_0(N)}{v_0}\right)^2 \left(\frac{L_{TCSA}}{2\pi N}\right)^{(5-K_{c+})/2}\right]. \quad (16)$$

In the above there is a quantity $\tilde{\Delta}_0(N)$. This is nothing but the value of the renormalized gap at the cutoff Λ of the theory, i.e., $\tilde{\Delta}_0(N) = \tilde{\Delta}(\Lambda)$. This is now almost the scaling function, Eq. (9). The only issue is that this is expressed in terms of the TCSA cutoff $\Lambda_{TCSA} = 2\pi v_0 N/L_{TCSA}$ that arises from our numerical treatment of the problem and not the effective bandwidth of the tube, Λ.

To determine the relationship between Λ and Λ_{TCSA} we begin by considering the bosonization formula giving the right/left moving fermion, $\psi_\pm^\dagger$, in terms of a normal ordered vertex operator of a boson:

$$\psi_\pm^\dagger(x) \sim : e^{i\phi_\pm(x)} : . \quad (17)$$

In writing this expression we have dropped prefactors such as Klein factors—for our purposes what matters is the normal ordered exponential. The key to the relationship between Λ and Λ_{TCSA} is found in the relation between the normal ordered vertex operator and its unnormal ordered counterpart:

$$: e^{i\phi_\pm(x)} : = \sqrt{\frac{2\pi}{L_{TCSA}}} e^{i\phi_\pm(x)} e^{1/2 \sum_{n>0}^{N} (1/n)} \approx \sqrt{\frac{2\pi}{L_{TCSA}}} e^{i\phi_\pm(x)} e^{\gamma/2} N^{1/2}, \quad (18)$$

where γ is the Euler constant and the factor $\sqrt{2\pi/L_{TCSA}}$ ensures the engineering dimension of the normal ordered vertex operator matches its anomalous dimension. The appearance of $N = L_{TCSA}\Lambda_{TCSA}/(2\pi v_0)$ reflects our use of the TCSA cutoff to regulate the UV divergences that normal ordering exhibits in the theory.

When we initially bosonize the theory, the total charge boson is normal ordered assuming $K_{c+} = 1$. When we rediagonalize the theory, absorbing the forward scattering part of the Coulomb interaction into the quadratic part of $\mathcal{H}$, we have to adjust the normal ordering to take into account $K_{c+} \neq 1$. We do so as follows:

$$: e^{\theta_{c+}/2} :_{K_{c+}=1} = \left(\frac{2\pi}{L_{TCSA}}\right)^{1/4} e^{\gamma/4} N_c^{1/4} e^{i\theta_{c+}/2} = \left(e^\gamma \frac{2\pi N_c}{L_{TCSA}}\right)^{(1-K_{c+})/4} : e^{\theta_{c+}/2} :_{K_{c+}\neq 1},$$

where the subscripts $: \cdot :_{K_{c+}}$ indicate the value of K_{c+} for which the normal ordering is being done. We use N_c instead of N as N_c governs the maximal energy in the total charge ($c+$) sector of the theory, not the entire theory itself. The two are related via

$$N_{c+} = \frac{N v_0}{4 v_{c+}}, \quad (19)$$

assuming an equipartition of energy between the four bosons in the theory. It is this difference in normal ordering prefactors that is absorbed into the bare coupling, Δ_0, when we bosonize the theory in Eq. (7).

$$\tilde{\Delta}_0 = \Delta_0 \left(e^\gamma \frac{2\pi N_{c+}}{L_{TCSA}}\right)^{(1-K_{c+})/4}. \quad (20)$$

Comparing the above with the relation $\tilde{\Delta}_0 = \Delta_0(\Lambda/v_{c+})^{(1-K_{c+})/4}$ then implies

$$\frac{\Lambda}{v_{c+}} = \frac{e^\gamma}{4 v_{c+}} \Lambda_{TCSA}. \quad (21)$$

We are now close to having a useful form for the scaling function. What remains is to determine how Λ, the effective bandwidth of theory, is related to the properties of the nanotube.

Λ reflects the largest energy scale in the low energy reduction of the tube. This energy scale is not the bandwidth of graphene ($\sim$9 eV), but rather some much smaller scale reflecting that the electrons on the tubes are delocalized around the tube's circumference. We thus take as an ansatz

$$\frac{\Lambda}{v_{c+}} = \frac{B}{d}, \quad (22)$$

where B is an $O(1)$ dimensionless constant and $d = 2R$ is the tube's diameter. We cannot directly determine this constant, but treat it as a fitting parameter, the only undetermined parameter of this approach. But we will see the same constant works over tubes with a wide variety of radii, different subbands within the same tube, and tubes in different dielectric environments. We will also see, as an important self-consistency check, that this same relation determines the finite bandwidth corrections to the excitonic gaps of higher subbands. Because the intuition behind this ansatz is of electron delocalization transverse to the main axis of the 1D system, we expect analogous relations to hold in other strongly correlated one dimensional materials. We consider this ansatz (and the fact that it works) to be one of the central results of this paper.

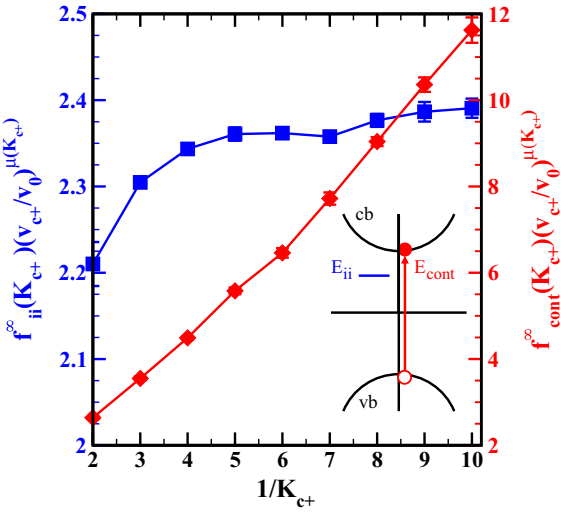

FIG. 1. (Color online) The scaling functions [see Eqs. (8) and (9)] for the E_{ii} excitons (excitons formed as a bound state of a hole in the i th valence subband and a particle in the i th conduction subband) and the particle-hole continuum, $E_{\rm cont}$. At $K_{c+} = 1$ (the noninteracting limit) these functions go to 2. Inset: Sketch of E_{ii} and $E_{\rm cont}$ excitations.

The scaling function can then be put in the form

$$E_{\rm exc} = f^{\infty}_{\rm exc}\tilde{\Delta}_0^{4/(5-K_{c+})} \times\left[1 + A(K_{c+})\left(\frac{\tilde{\Delta}(\Lambda)}{v_0}\right)^2\left(\frac{v_0}{\Lambda}\right)^{(5-K_{c+})/2}\right];$$
$$A(K_{c+}) = \frac{8\alpha(K_{c+})}{(5-K_{c+})^2}\left(\frac{e^{\gamma}}{4}\right)^{(5-K_{c+})/2}, \qquad (23)$$

where $\alpha(K_{c+})$ is defined in the RG equation [Eq. (13)]. The final detail to be discussed is the numerical determination of the coefficients $f^{\infty}_{\rm exc}$ and $A(K_{c_+})$. To extract these, we numerically study the full Hamiltonian, $\mathcal{H}_0 + \mathcal{H}_{\rm gap}$, using the previously mentioned TCSA-NRG. The coefficients f^{∞} for the excitons and particle-hole continuum were already determined in Ref. [21] (where details of the numerical analysis can be found) but because these are central quantities for the purpose of analyzing experimental data, we reproduce them here in Fig. 1 where they are plotted as a function of K_{c+}.

We see the scaling function for E_{ii} is relatively flat as a function of K_{c+} while that of $E_{\rm cont}$ varies comparatively sharply. In the limit K_{c+} tends to 1 (the noninteracting limit), the scaling function f^{∞}_{ii} tends to 2 (i.e., the exciton energy is that of the bare (noninteracting) particle-hole continuum gap). In the limit K_{c+} tends to 0, $f^{\infty}_{ii} \propto K_{c+}^{-1/5}$, only going to infinity slowly. In contrast, $f^{\infty}_{\rm cont}$ grows much more quickly, going as K_{c+}^{-1}. We have thus quantified the general observation [33] that the renormalization of the single particle gap due to Coulomb interactions is much more marked than that of the excitons. It is also much stronger than has been suggested in random-phase-approximation-type computations [47]. We immediately infer that the binding energy of the exciton as a fraction of the exciton energy grows as $K_{c+}^{-4/5}$ as $K_{c+} \to 0$. We will see in the next section that this leads to very large predicted binding energies for the tubes which we study using this approach (see Figs. 5 and 6).

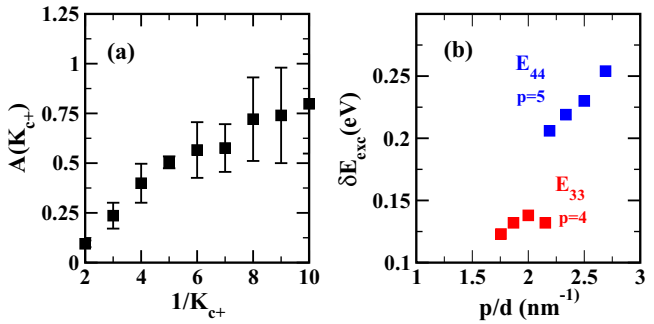

FIG. 2. (Color online) (a) The function $A(K_{c+})$ giving the size of the finite bandwidth correction to E_{ii}. (b) The size of this correction, $\delta E_{\rm exc}$, for the excitons, E_{33} and E_{44}, of the four tubes studied in Ref. [23].

Also shown in Fig. 2 [panels (a) and (b)] are numerical data demonstrating the size of the finite bandwidth corrections to the tubes. In Fig. 2(a) we plot the coefficient $A(K_{c+})$ governing how the finite bandwidth correction affects the excitonic energies. And in Fig. 2(b) we plot the overall size of the finite bandwidth correction for excitons in the third and fourth subbands in the tubes studied in Ref. [23]. We plot it for these tubes in particular because the bandwidth correction here is large (on the order of several hundred meV).

III. ANALYSIS OF EXPERIMENTAL DATA

We now examine how this theoretical approach fares in predicting the excitonic data of Refs. [23] and [24]. These papers present excitonic gaps of tubes for a wide range of diameters and subbands as well as different dielectric environments. We note that despite representing a wide collection of tubes, the effective K_{c+} for this collection has a comparatively small range, $0.16 < K_{c+} < 0.26$. This might make one think that the test of our approach is rather limited. However for a given tube, the predicted excitonic gap will vary by up to 10% for this range of K_{c+}'s whereas, as we will see, the accuracy of our predictions is typically within a few percent. Another aspect of the scaling form that is similarly tested is its accuracy in predicting the dependency of excitonic gaps on tube diameter. We stress that the ansatz taken in Eq. (22) for the relation between the cutoff of the tube and its diameter is a key part of this analysis and proves to be remarkably good. Getting this wrong (say by taking a single uniform diameter-independent cutoff) would lead to deviations to the gaps on the order of 10%, whereas again we find agreement between our theory and experiment to be on the order of a few percent.

A. Excitonic gaps

Let us now turn to the data. In Ref. [23] measurements were performed on a set of four larger diameter tubes (d running from 1.86 to 2.14 nm). In each of the four tubes, the first four single photon excitons, E_{ii}, $i = 1, \ldots, 4$, were measured. E_{33} and E_{44} were studied by suspending the

nanotubes and using Rayleigh scattering spectroscopy. In these measurements the relevant dielectric constant was $\kappa = 1$. These same tubes were then printed onto a silicon wafer where source and drain electrons were patterned. This enabled E_{11} and E_{22} to be measured by a complimentary technique, Fourier-transform photoconductivity. In this configuration the effective dielectric constant of the tubes is the average of air and silicon dioxide, $\kappa = (1 + \kappa_{SiO_2})/2 = 2.45$, a result easily derived from considering the effective potential between two charges confined to the interface of two media with different dielectric constants. To determine the appropriate value of the Luttinger parameter for these tubes, we need to specify $k_{\min}$. The length, L, of the tubes of Ref. [23] was typically $L \sim 2\ \mu$m (a number equal to the mean free path [48]), l_{mf}, and so we take $k_{\min} = 2\pi/L$. This leads to a Luttinger parameter of $K_{c+} = 0.16$ for the tubes suspended in air and $K_{c+} = 0.24$ for the tubes printed onto the silicon substrate. The smaller K_{c+} for the suspended tubes indicates the action of a considerably stronger effective Coulomb interaction for the tubes in this configuration.

In Ref. [24] the single photon excitons, E_{11}, were measured for a set of 13 tubes with diameters between 0.78 and 1.18 nm. The tubes were embedded in a polymaleic acid/octyl vinyl ether (PMAOVE) matrix with an effective dielectric constant of $\kappa = 2.5$ [25]. The excitons were measured using two photon spectroscopy—thus the E_{2g} photons were also studied in this work but will not be considered here. As the length of tubes in the PMAOVE matrix was reported to be $L = 400$ nm [49], far smaller than l_{mf}, we take $k_{\min} = 2\pi/L$ here. This leads to a Luttinger parameter of $K_{c+} = 0.26$. Because of the logarithmic dependence of K_{c+} upon $k_{\min}$, K_{c+} is relatively insensitive to $O(1)$ changes of $k_{\min}$.

As an ingredient to our analysis of the data in Refs. [23] and [24] we need to determine the bare value of the gap, Δ_0, for each tube. We do so with a tight-binding model based on wrapping a honeycomb lattice of nearest neighbor spacing $a_0 = 1.42$ Å and hopping parameter $t = 3.0$ eV. We do not attempt to include curvature, twist, or stress corrections to Δ_0 (for a discussion of these see Refs. [50] and [51]) although for small radius tubes such corrections may not be insignificant. But to be able to do so would require detailed characterization of the tubes in their environment, which is not available.

As we have explained the treatment has one fitting parameter: the constant B governing the relationship between the effective bandwidth of the nanotube and the tube's diameter, d. To find this constant B we focus on the four E_{11} excitonic gaps reported in Ref. [23]. We focus on these gaps because for these the correction due to finite bandwidth [the second term in Eq. (9)] can safely be ignored. When we fit Eq. (22) we find $B \sim 0.51$. We will henceforth use this value for B to determine theoretical values of the gaps for all the other single photon excitons reported in Refs. [23] and [24].

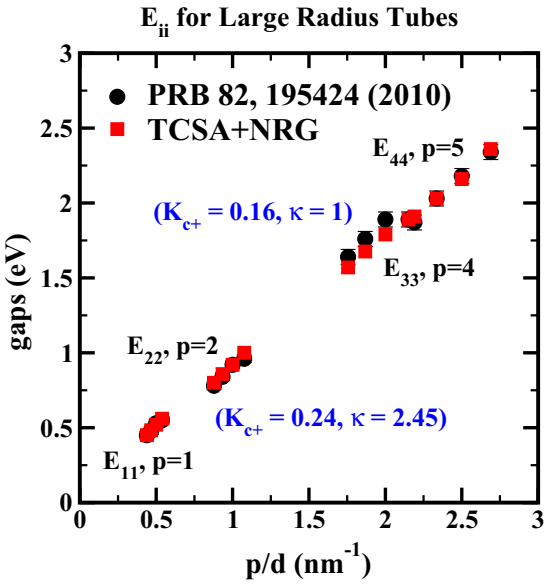

FIG. 3. (Color online) Comparison of the measured exciton gaps of the first four subbands, E_{ii}, $i = 1,2,3,4$ ($p = 1,2,4,5$ in the notation of Ref. [33]) of four nanotubes with different chiralities (as reported in Ref. [23]) with gaps derived from the scaling function determined by TCSA-NRG.

Remarkably this relationship between the bandwidth and the tube's diameter leads to excellent values for the other excitonic gaps considered in this study. To demonstrate this we first consider all (16) of the gaps reported in Ref. [23]. Our results for the gaps are presented in Table I and Fig. 3. We see that the agreement between the theoretically predicted values of the gaps and the corresponding experimentally measured values is better than 2% for the E_{11}, E_{22}, E_{44}, and one of the E_{33} gaps and on the order of 5% for the remaining E_{33} gaps. The relatively good agreement found for the E_{33} and E_{44} gaps is a result of taking into account the finite bandwidth corrections coming from the subleading term in Eq. (9) where the corrections for E_{33} and E_{44} are large [>100 meV—see Fig. 2(b)]. These corrections in Eq. (9), inasmuch as they are proportional to $\tilde{\Delta}_0^2/\Lambda^{(5-K_{c+})/2}$, depend in turn upon our identification of Λ with the tube diameter. It is an important consistency check for this ansatz in Eq. (22) that the computed corrections lead to a good match between the experiment and theory.

We find similar good agreement in our theoretical analysis of the E_{11} excitons reported in Ref. [23]. Using the same

TABLE I. Comparison of the experimental and theoretical values of E_{ii} of the large radius tubes reported in Ref. [23]. All energies are in units of eV.

(n,m)	K_{c+}, $i = 1,2$	$\Delta_{0,11}$	$E_{11,\text{Theor.}}$	$E_{11,\text{Expt.}}$	$\Delta_{0,22}$	$E_{22,\text{Theor.}}$	$E_{22,\text{Expt.}}$	K_{c+}, $i = 3,4$	$\Delta_{0,33}$	$E_{33,\text{Theor.}}$	$E_{33,\text{Expt.}}$	$\Delta_{0,44}$	$E_{44,\text{Theor.}}$	$E_{44,\text{Expt.}}$
(14,13)	0.241	0.232	0.56	0.55	0.466	1.00	0.96	0.156	0.913	1.89	1.89	1.139	2.36	2.34
(19,14)	0.244	0.190	0.45	0.45	0.377	0.80	0.78	0.158	0.759	1.57	1.64	0.921	1.91	1.87
(17,12)	0.242	0.216	0.52	0.53	0.427	0.92	0.92	0.157	0.863	1.79	1.89	1.039	2.16	2.18
(18,13)	0.243	0.202	0.48	0.48	0.400	0.86	0.84	0.158	0.808	1.68	1.76	0.977	2.03	2.03

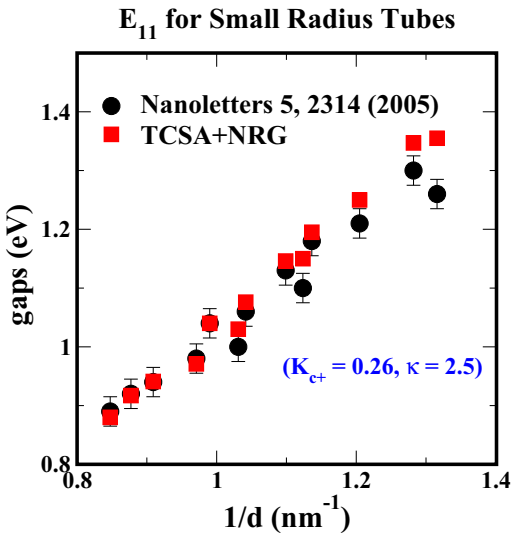

FIG. 4. (Color online) Comparison of the measured exciton gaps of the first subband, E_{11}, in a set of small radius tubes as reported in Ref. [24] with those computed using TCSA-NRG.

relationship as before of the bandwidth to the tube diameter (i.e., the coefficient B), we plot our predicted values for E_{11} against those measured in Ref. [24] in Fig. 4. We see that in general we get good agreement between theory and experiment for these small radius tubes (see Table II). What discrepancies we do see (which are most pronounced for the tubes with the smallest radius) are a likely consequence of omitted curvature, strain, and twist effects on the bare gap, Δ_0, for this set of tubes (which we note again we cannot directly estimate).

B. Excitonic binding energies

We finally consider the excitonic binding energies of the E_{11} excitons reported in Refs. [23] and [24]. We first plot in Fig. 5 the excitonic binding energies as a function of K_{c+}^{-1}. The binding energies are presented as a fraction of the exciton gap. We see that for K_{c+}^{-1} large, the binding energies can be many multiples of the excitonic gap itself.

TABLE II. Comparison of the experimental and theoretical values of E_{11} of the small radius tubes reported in Ref. [24].

(n,m)	K_{c+}	$\Delta_{0,11}$	$E_{11,\text{Theor.}}$	$E_{11,\text{Expt.}}$
(8,3)	0.26	0.562	1.35	1.30
(6,5)	0.26	0.564	1.36	1.26
(7,5)	0.26	0.523	1.25	1.21
(10,2)	0.26	0.499	1.20	1.18
(9.4)	0.26	0.478	1.15	1.13
(7,6)	0.26	0.479	1.15	1.1
(8,6)	0.26	0.448	1.08	1.06
(11,3)	0.26	0.434	1.04	1.04
(9,5)	0.26	0.436	1.03	1.00
(8,7)	0.26	0.416	0.97	0.98
(9,7)	0.26	0.392	0.94	0.94
(12,4)	0.26	0.383	0.92	0.92
(11,6)	0.26	0.367	0.88	0.89

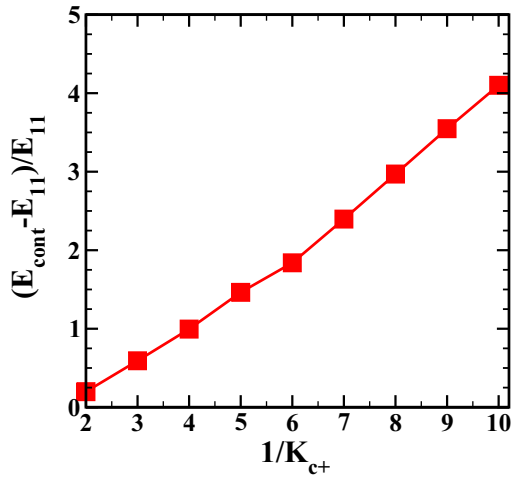

FIG. 5. (Color online) Binding energy of the excitons as a function of K_{c+}^{-1} expressed in units of the excitonic gap.

As K_{c+}^{-1} decreases, the fractional exciton binding energy decreases linearly in line with the linear decrease of E_{cont} [as seen in Fig. 1(a)]. In Fig. 6 we plot the excitonic binding energies for the E_{11} excitons. Given that $K_{c+}^{-1} \sim 4$ for these gaps, we see that from Fig. 5 the binding energies roughly equal the gaps, E_{11}, themselves. The estimates of the binding energies for the E_{11} excitons of Ref. [24] are considerably larger than those in Ref. [39], a consequence of our much larger estimate here of the renormalized band gaps. It would thus be of considerable interest if these band gaps could be measured directly. But this is a difficult task as the standard method for measuring the particle-hole continuum, scanning tunneling microscopy [52], involves placing the tubes on a metallic substrate. The consequent screening of the Coulomb interaction leads to values of K_{c+} near to 1, far away from values of K_{c+} appropriate for the excitons measured in Refs. [23] and [24].

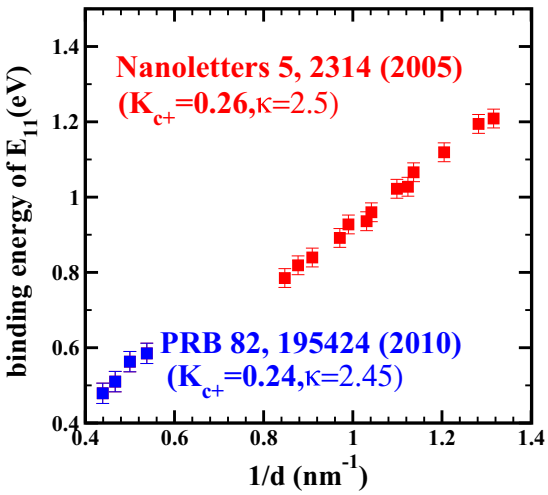

FIG. 6. (Color online) The predicted binding energies of the excitonic gaps, E_{11}, reported in Refs. [23] and [24].

IV. CONCLUSIONS

In summary, we have presented a quantum field theoretical formalism able to predict the absolute magnitudes of optically active excitons in semiconducting carbon nanotubes over a wide range of diameters, subbands, and dielectric environments. This method involves a single fitting parameter, B, relating the effective bandwidth of the tube to the tube's diameter. Once this parameter is in hand, a simple scaling function yields the excitonic gaps for arbitrary nanotubes. We have compared the predictions of this formalism with the excitonic data of Refs. [23] and [24] and have found good agreement. Finally we believe the methodology introduced here can be used to determine the absolute magnitude of excitation gaps in other one-dimensional strongly correlated materials.

ACKNOWLEDGMENTS

The research herein was carried out in part in the CMPMS Department (R.M.K. and J.M.) and at the Center for Functional Nanomaterials (MS), Brookhaven National Laboratory, which is supported by the U.S. Department of Energy, Office of Basic Energy Sciences, under Contract No. DE-AC02-98CH10886.

APPENDIX A: BOSONIZATION CONVENTIONS

In this section we outline our bosonization conventions. We follow those of Ref. [12] with a few adjustments that will be noted. We begin by writing the four species of fermions, $\psi_{\alpha\sigma}$ (characterized by the quantum numbers for spin $\sigma = \uparrow / \downarrow$ and valley $\alpha = K, K'$), in terms of their right and left moving parts:

$$\psi_{\alpha\sigma} \sim \psi_{+\alpha\sigma} e^{ik_{F_\alpha} x} + \psi_{-\alpha\sigma} e^{-ik_{F_\alpha} x}. \tag{A1}$$

We in turn bosonize these right and left moving fermions in the standard way:

$$\psi_{r\alpha\sigma} = \frac{\kappa_{\alpha\sigma}}{\sqrt{2\pi}} : e^{i\phi_{r\alpha\sigma}} : \quad r = +,- = \text{right,left}. \tag{A2}$$

The extra $1/\sqrt{2\pi}$ in comparison to Ref. [12] here arises because we use conformal conventions in how we write the normal ordered vertex function in terms of its non-normal ordered counterpart [see Eq. (18)]. Here $\kappa_{\alpha\sigma}$ are Klein factors satisfying

$$\{\kappa_{j\alpha}, \kappa_{i\beta}\} = 2\delta_{ij}\delta_{\alpha\beta}. \tag{A3}$$

In terms of these four Bose fields, four new Bose fields are defined (effectively separating charge and spin):

$$\begin{aligned}
\phi_{rc+} &= \tfrac{1}{2}(\phi_{rK\uparrow} + \phi_{rK\downarrow} + \phi_{rK'\uparrow} + \phi_{rK'\downarrow});\\
\phi_{rs+} &= \tfrac{1}{2}(\phi_{rK\uparrow} - \phi_{rK\downarrow} + \phi_{rK'\uparrow} - \phi_{rK'\downarrow});\\
\phi_{rc-} &= \tfrac{1}{2}(\phi_{rK\uparrow} + \phi_{rK\downarrow} - \phi_{rK'\uparrow} - \phi_{rK'\downarrow});\\
\phi_{rs-} &= \tfrac{1}{2}(\phi_{rK\uparrow} - \phi_{rK\downarrow} - \phi_{rK'\uparrow} + \phi_{rK'\downarrow}).
\end{aligned} \tag{A4}$$

The first and second bosons in the above describe total charge and spin fluctuations, respectively. The latter two bosons, ϕ_{rc-} and ϕ_{rs-}, describe relative charge and spin fluctuations between the two valleys of the nanotube. We note that our definition of ϕ_{Lc-} differs by a minus sign from Ref. [12] [this sign was introduced to exhibit explicitly an underlying $SO(8)$ symmetry in a related model describing two-leg Hubbard ladders].

From these chiral bosons, one can define pairs of conjugate bosons in the standard fashion:

$$\begin{aligned}
\varphi_i &= \phi_{Ri} + \phi_{Li};\\
\theta_i &= \phi_{Ri} - \phi_{Li},
\end{aligned} \tag{A5}$$

which obey the commutation relations,

$$[\varphi(x), \theta(x')] = -i4\pi\,\Theta(x' - x), \tag{A6}$$

where $\Theta(x - x')$ is the Heaviside step function.

In terms of these variables the kinetic part of the Hamiltonian can be written

$$\mathcal{H}_{\text{kin}} = \frac{v_0}{8\pi} \sum_{i=c\pm,s\pm} \{(\partial_x \varphi_i)^2 + (\partial_x \theta_i)^2\}, \tag{A7}$$

while H_{Coulomb} becomes

$$H_{\text{Coulomb}} = \frac{v_0}{8\pi K_{c+}^2} \int dx (\partial_x \theta_{c+})^2 \tag{A8}$$

(see Refs. [19] and [20]). For H_{Coulomb} we have dropped terms that are marginal. We have explicitly checked that such terms lead only to very small corrections to the excitonic spectrum (less than 1%) [21]. Putting the above together, we obtain Eq. (4) of the main text:

$$H_0 = \frac{1}{8\pi} \sum_{i=c\pm,s\pm} v_i \left\{ K_i (\partial_x \varphi_i)^2 + \frac{1}{K_i} (\partial_x \theta_i)^2 \right\}. \tag{A9}$$

Finally with these bosonization conventions, $\mathcal{H}_{\text{gap}}$ reduces to

$$\mathcal{H}_{\text{gap}} = \frac{4\tilde{\Delta}_0}{\pi} \left[\prod_i \cos\left(\frac{\theta_i}{2}\right) + \prod_i \sin\left(\frac{\theta_i}{2}\right) \right], \tag{A10}$$

as written in Eq. (7) of the main text.

APPENDIX B: CORRECTIONS TO EXCITONIC ENERGIES DUE TO INTERSUBBAND INTERACTIONS

In this section we will compute the corrections to excitonic energies due to interactions between subbands. We will demonstrate that they are proportional to v_0^4/c^4 where c is the speed of light and so are small.

Consider an excitonic excitation in subband i with energy Δ_i. The forward scattering portion of the intersubband Coulomb interaction (as with the intrasubband interactions, the strongest part of the Coulomb interaction) takes the form

$$H_{\text{inter}CI} = \sum_{i>j} \int dx dx' \rho_i(x) V_c(x - x') \rho_j(x'), \tag{B1}$$

where ρ_i is the density in the i th subband. In the long wavelength limit this can be rewritten as

$$\begin{aligned}
H_{\text{inter}CI} &= \sum_{i>j} \int dx \rho_i(x) \rho_j(x) V_c(k=0)\\
&= \Gamma \sum_{i>j} \int dx \partial_x \theta_{c+,i}(x) \partial_x \theta_{c+,j}(x),
\end{aligned} \tag{B2}$$

where $\Gamma = v_0/(8\pi K_{c+})$ and we have used in the second line the bosonized expressions for the electron densities in the subbands.

In second order perturbation theory the correction to Δ_i takes the form

$$\delta\Delta_i = \Gamma^2 \sum_n \frac{|\langle\Delta_i| \otimes \langle GS_j|H_{\text{inter}CI}|GS_i\rangle \otimes |\Delta_{n,j}\rangle|^2}{\Delta_i - \Delta_{n,j}}, \quad \text{(B3)}$$

where $|\Delta_{n,j}\rangle$ is some excitation in the j th subband with parity odd symmetry (i.e., odd under $\theta_{c+,j} \to -\theta_{c+,j}$) with energy $\Delta_{n,j}$. The lowest energy such excitations are the one-photon excitons in subband j. The state $|GS_j\rangle$ is the ground state of the j th subband. The matrix elements that we have to evaluate in this sum take the form

$$\langle\Delta_i|\rho_i(x)|GS_i\rangle = M_i e^{ip_i x} p_i;$$
$$\langle\Delta_{n,j}|\rho_j(x)|GS_j\rangle = M_{n,j} e^{ip_j x} p_{j,n}, \quad \text{(B4)}$$

where M_i and $M_{n,j}$ are $O(1)$ constants (as can be verified numerically) and $p_i/p_{n,j}$ are the momenta of the excitations $|\Delta_i\rangle/|\Delta_{n,j}\rangle$. Thus the energy correction takes the form

$$\delta\Delta_i = \sum_n \frac{v_0^2 p_1^4 |M_i|^2 |M_{j,n}|^2 \Gamma^2}{(\Delta_i^2 + v_0^2 p_i^2)(\Delta_i - E_{n,j})}. \quad \text{(B5)}$$

As one can see this correction vanishes as the momentum of the exciton goes to zero. Typically the momentum of an optically excited exciton will be equal to Δ_i/c, implying that $\delta\Delta_i$ is proportional to $(v_0/c)^4$ and so is very small.

[1] D. C. Dender, P. R. Hammar, D. H. Reich, C. Broholm, and G. Aeppli, Phys. Rev. Lett. **79**, 1750 (1997).
[2] M. Oshikawa and I. Affleck, Phys. Rev. Lett. **79**, 2883 (1997); I. Affleck and M. Oshikawa, Phys. Rev. B **60**, 1038 (1999).
[3] F. H. L. Essler, Phys. Rev. B **59**, 14376 (1999).
[4] I. Kuzmenko and F. H. L. Essler, Phys. Rev. B **79**, 024402 (2009).
[5] F. H. L. Essler and R. M. Konik, Phys. Rev. B **75**, 144403 (2007); R. M. Konik, F. H. L. Essler, and A. M. Tsvelik, *ibid.* **78**, 214509 (2008).
[6] F. H. L. Essler, A. M. Tsvelik, and G. Delfino, Phys. Rev. B **56**, 11001 (1997).
[7] S. C. Furuya and M. Oshikawa, Phys. Rev. Lett. **109**, 247603 (2012).
[8] A. B. Zamolodchikov, Int. J. Mod. Phys. A **04**, 4235 (1989).
[9] R. Coldea, D. A. Tennant, E. M. Wheeler, E. Wawrzynska, D. Prabhakaran, M. Telling, K. Habicht, P. Smeibidl, and K. Kiefer, Science **327**, 177 (2010).
[10] F. H. L. Essler and A. M. Tsvelik, Phys. Rev. B **65**, 115117 (2002).
[11] F. H. L. Essler and A. M. Tsvelik, Phys. Rev. Lett. **88**, 096403 (2002).
[12] H. H. Lin, L. Balents, and M. P. A. Fisher, Phys. Rev. B **58**, 1794 (1998); R. M. Konik and A. W. W. Ludwig, *ibid.* **64**, 155112 (2001).
[13] M. J. Bhaseen, F. H. L. Essler, and A. Grage, Phys. Rev. B **71**, 020405 (2005).
[14] L. S. Levitov and A. M. Tsvelik, Phys. Rev. Lett. **90**, 016401 (2003).
[15] C. L. Kane and M. P. A. Fisher, Phys. Rev. B **46**, 15233 (1992).
[16] Chang-Yu Hou, Eun-Ah Kim, and Claudio Chamon, Phys. Rev. Lett. **102**, 076602 (2009).
[17] A. Agarwal, S. Das, S. Rao, and D. Sen, Phys. Rev. Lett. **103**, 026401 (2009); A. Rahmani, C.-Y. Hou, A. Feiguin, M. Oshikawa, C. Chamon, and I. Affleck, Phys. Rev. B **85**, 045120 (2012).
[18] W. DeGottardi, T.-C. Wei, and S. Vishveshwara, Phys. Rev. B **79**, 205421 (2009).
[19] R. Egger and A. O. Gogolin, Eur. Phys. J. B **3**, 281 (1998).
[20] C. L. Kane, L. Balents, and M. P. A. Fisher, Phys. Rev. Lett. **79**, 5086 (1997).
[21] R. M. Konik, Phys. Rev. Lett. **106**, 136805 (2011).
[22] L. Wang, H. Liu, R. M. Konik, J. A. Misewich, and S. S. Wong, Chem. Soc. Rev. **42**, 8134 (2013).
[23] M. Y. Sfeir, J. A. Misewich, S. Rosenblatt, Y. Wu, C. Voisin, H. Yan, S. Berciaud, T. F. Heinz, B. Chandra, R. Caldwell, Y. Shan, J. Hone, and G. L. Carr, Phys. Rev. B **82**, 195424 (2010).
[24] G. Dukovic, F. Wang, D. Song, M. Y. Sfeir, T. Heinz, and L. Brus, Nano Lett. **5**, 2314 (2005).
[25] F. Wang, G. Dukovic, L. E. Brus, and T. F. Heinz, Science **308**, 838 (2005).
[26] S. M. Bachilo, M. S. Strano, C. Kittrell, R. H. Hauge, R. E. Smalley, and R. B. Weisman, Science **298**, 2361 (2002).
[27] P. T. Araujo, S. K. Doorn, S. Kilina, S. Tretiak, E. Einarsson, S. Maruyama, H. Chacham, M. A. Pimenta, and A. Jorio, Phys. Rev. Lett. **98**, 067401 (2007).
[28] M. J. O'Connell, S. M. Bachilo, C. B. Huffman, V. C. Moore, M. S. Strano, E. H. Haroz, K. L. Rialon, P. J. Boul, W. H. Noon, C. Kittrell, J. Ma, R. H. Hauge, R. B. Weisman, and R. E. Smalley, Science **297**, 593 (2002).
[29] J.-C. Charlier, X. Blase, and S. Roche, Rev. Mod. Phys. **79**, 677 (2007).
[30] T. J. Ando, Phys. Soc. Jpn. **66**, 1066 (1997)
[31] M. Rohlfing and S. G. Louie, Phys. Rev. B **62**, 4927 (2000).
[32] V. Perebeinos, J. Tersoff, and P. Avouris, Phys. Rev. Lett. **92**, 257402 (2004).
[33] C. L. Kane and E. J. Mele, Phys. Rev. Lett. **93**, 197402 (2004).
[34] L. Yang, M. Cohen, and S. G. Louie, Nano Lett. **7**, 3112 (2007).
[35] L. Wirtz, A. Marini, and A. Rubio, Phys. Rev. Lett. **96**, 126104 (2006); J. S. Lauret, R. Arenal, F. Ducastelle, A. Loiseau, M. Cau, B. Attal-Tretout, and E. Rosencher, *ibid.* **94**, 037405 (2005); R. Arenal, O. Stéphan, M. Kociak, D. Taverna, A. Loiseau, and C. Colliex, *ibid.* **95**, 127601 (2005).
[36] H. Akiyama, J. Phys.: Condens. Matter **10**, 3095 (1998).
[37] V. Perebeinos, J. Tersoff, and P. Avouris, Nano Lett. **5**, 2495 (2005).
[38] J. Maultzsch, R. Pomraenke, S. Reich, E. Chang, D. Prezzi, A. Ruini, E. Molinari, M. S. Strano, C. Thomsen, and C. Lienau, Phys. Rev. B **72**, 241402(R) (2005); D. Kammerlander, D. Prezzi, G. Goldoni, E. Molinari, and U. Hohenester, Phys. Rev. Lett. **99**, 126806 (2007).
[39] J. Deslippe, M. Dipoppa, D. Prendergast, M. V. O. Moutinho, R. B. Capaz, and S. G. Louie, Nano Lett. **9**, 1330 (2009).

[40] S. Coleman, Phys. Rev. D **11**, 2088 (1975).
[41] Al. B. Zamolodchikov, Nucl. Phys. B **348**, 619 (1991).
[42] V. P. Yurov and Al. B. Zamolodchikov, Int. J. Mod. Phys. A **06**, 4557 (1991).
[43] K. Wilson, Rev. Mod. Phys. **47**, 773 (1975).
[44] R. M. Konik and Y. Adamov, Phys. Rev. Lett. **98**, 147205 (2007).
[45] G. Watts, Nucl. Phys. B **859**, 177 (2012); P. Giokas and G. Watts, arXiv:1106.2448.
[46] G. Feverati, K. Graham, P. A. Pearce, G. Toth, and G. Watts, arXiv:hep-th/0612203; M. Lencsés and G. Takács, J. High Energy Phys. 09 (2014) 052.
[47] H. Sakai, H. Suzuurab, and T. Ando, Physica E **22**, 704 (2004).
[48] M. S. Purewal, B. H. Hong, A. Ravi, B. Chandra, J. Hone, and P. Kim, Phys. Rev. Lett. **98**, 186808 (2007).
[49] G. Dukovic, B. E. White, Z. Zhou, F. Wang, S. Jockusch, M. L. Steigerwald, T. F. Heinz, R. A. Friesner, N. J. Turro, and L. E. Brus, J. Am. Chem. Soc. **126**, 15269 (2004).
[50] A. Kleiner and S. Eggert, Phys. Rev. B **63**, 073408 (2001).
[51] L. Yang, M. P. Anantram, J. Han, and J. P. Lu, Phys. Rev. B **60**, 13874 (1999).
[52] H. Lin, J. Lagoute, V. Repain, C. Chacon, Y. Girard, J.-S. Lauret, F. Ducastelle, A. Loiseau, and S. Rousset, Nat. Mater. **9**, 235 (2010).